Modelling and Simulation of the Lifetime of Saturated Batteries in Real Operating Conditions

VODOUNNOU Edmond Claude, NOUNANGNONHOU Cossi Telesphore, AHOUANSOU Houêchénè Roger, SEMASSOU Guy Clarence, Adam IMOROU KARIM

Laboratory of Energetics and Applied Mechanics (LEMA), Polytechnic School of Abomey-Calavi (EPAC), 01BP 2009 Cotonou; University of Abomey-Calavi (UAC), Bénin

Abstract This work consists of predicting the lifetime of stationary batteries, in particular the lead acid battery, under real operating conditions. This was made possible by the mathematical model of Schiffer et al, which takes into account the corrosion, degradation of the active material, depth of discharge, acid stratification, and gassing that take place inside the battery during its operation. The model determines the remaining capacity coefficient of the battery for a given operating time. This coefficient allowed to deduce the end of life of the battery. Indeed, the battery is at the end of its life when its remaining capacity is to 20% of the initial value of its capacity. The simulation results show that over 5 years of simulation, the capacity coefficient of the battery studied drops from 1.75 to 0.35 after 3 years 153 days of operation, i.e. 20% of the initial capacity coefficient (1.75), which allows to conclude that the end of life of this battery is reached after 3 years 153 days of operation.

Introduction

Today, a large part of the world's energy production is provided by fossil fuels. The exploitation of these fossil sources is not without consequences on the environment. Among these dangers are: global warming, destruction of the ozone layer, pollution, etc. To limit the use of fossil fuels, it is necessary to turn to renewable energies. Renewable energies are energies whose sources are inexhaustible, available and free. The operation of an electrical system from renewable energies, such as wind or solar energy, is often limited by the variable and intermittent nature of these energies [1]. To ensure continuity in the production of energy, it is therefore necessary to use energy storage systems [1]. Energy storage consists of storing energy in a device, in order to use it later. For photovoltaic systems for example, during periods low consumption, the excess energy produced is stored in the battery and during the peak period or to compensate for the intermittency of the source (sun), the energy stored is used to satisfy the energy demand. Today we record several energy storage models, these are: mechanical, thermal, chemical and electrochemical etc. In this study, we are interested in electrochemical storage. Electrochemical energy storage in batteries is more attractive because the systems are compact, easy to deploy, cost-effective, and provide nearly instantaneous response to both energy storage and release [1]. Stationary batteries today occupy a significant part of the initial investment and the costs generated by their replacement are not negligible. It is clear that batteries very often reach the end of their life well before the durations defined by the manufacturer. The life of a stationary battery depends on the number of cycles and the depth of discharge. However, there are phenomena which accelerate the reduction of the duration of this life:

anodic corrosion, degradation of positive active mass and loss of adhesion of the grids, irreversible formation of lead sulphate, short circuits, water loss and acid stratification [2]. Given the importance of these batteries to ensure the continuity of the supply of electrical energy, as well as their cost in the whole system, the study of these systems is of great interest. We are specifically interested here in lead-acid batteries integrated in renewable energy systems. The objective of this work is to develop a simulation tool to predict the life of a stationary battery in real operating conditions. Specifically, we have identified the factors that influence battery life under real-world conditions, we reviewed existing models on the lifespan of the different battery technologies in order to retain and possibly improve a model and then proceed with the implementation of the selected model. From our results, it appears that the lifetime of the AGM battery is 7 to 10 years for a temperature of 20°C. For a temperature of 25°C, we obtained a lifespan of 3 years 153 days. The results obtained underestimate the battery life, and this is due to non-compliance with the conditions of use of the battery. The results also show that the temperature has a negative influence on the performance (voltage and state of charge) of the battery. So when the temperature rises, the battery struggles to reach maximum charges. Finally we found that at higher temperatures the capacity of the battery increases and this result is supported by the data sheet of the battery. However, under no circumstances should these batteries be placed in a hot place to take advantage of this increase in capacity. The side effects mentioned above are much more harmful.

Materials and Methods
Description of the Schiffer et al. model
The aging model of Schiffer et al. allows to estimate the remaining capacity of lead acid batteries after a period of operation.
The model takes as input:
- The ambient temperature over the operating period;
- The charge and discharge current I.

With these inputs, the model proceeds to estimate the remaining capacity in four steps, namely:
a.   Calculation of the cell voltage U and the state of charge SOC;
b.   Calculation of the corrosion parameters (corrosion voltage, corrosion layer thickness) and the degradation parameters, the impact of the state of charge, the impact of the acid stratification;
c.   Updating of battery parameters such as resistance and capacity;
d.   Calculation of the remaining capacity.

In the following, we present each of the above-mentioned steps. The simplified flowchart of the model is as follows:
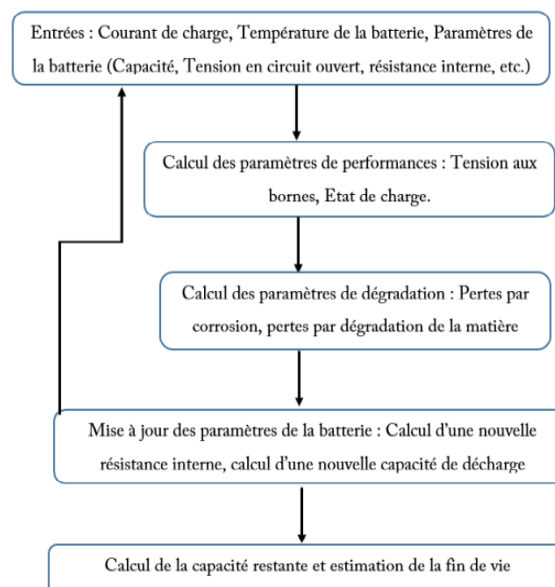

Figure 1: Flow chart of the Schiffer et al model

Charge transfer model

The charge transfer model is used to calculate the SOC of the battery. The state of charge is calculated by integrating the difference between the current I and the gassing current divided by the nominal capacity [1]. The state of charge is the most important representation of the battery's condition.

$$SOC(t) = SOC(0) + \int_0^t \frac{I(t) - I_{gazage}(t)}{C_N} dt \tag{1}$$

Gassing current

The gassing current is determined from the Tafel approximation [1]:

$$I_{gaz} = \frac{C_N}{100Ah} I_{gaz,0} \cdot \exp\left[c_U\left(U - U_{gaz,0}\right) + c_T(T - T_{gaz,0})\right] \tag{2}$$

Where, C_N is the rated capacity, $I_{gas,0}$ the normalized gassing current, C_U the voltage coefficient, $U_{gas,0}$ the rated gassing voltage, C_T the temperature coefficient, U is the battery cell voltage, and T the battery temperature.

Voltage model

Voltage is a critical parameter for corrosion and state of charge. The cell voltage is calculated from the modified Schiffer formula [1]:

During charging, I > 0 we have:

$$U(t) = U_0 - g.DOD(t) + \rho_C \frac{I(t)}{C_N} + \rho_C M_C \frac{I(t)}{C_N} \frac{SOC(t)}{C_c - SOC(t)} \tag{3}$$

- During the discharge I < 0 on a :

$$U(t) = U_0 - g.DOD(t) + \rho_d \frac{I(t)}{C_N} + \rho_d M_d \frac{I(t)}{C_N} \frac{DOD(t)}{C_d - DOD(t)} \tag{4}$$

U(t) is the cell terminal voltage, U_0 is the open-circuit cell voltage, g is an electrolyte proposal, SOC(t) is the battery state of charge, DOD(t) = 1-SOC(t) is the depth of discharge, ρ_c and ρ_d [ΩAh] are internal resistances during charge and discharge respectively, C_N is the nominal capacity of the battery, M_c and M_d are transfer overvoltage coefficients during charge and discharge respectively, Cc and Cd are normalized capacities during charge and discharge respectively.

Aging model

Two aging mechanisms are modeled, corrosion and degradation of the active material. An overview of how they are treated is described in this section.

Corrosion model

In the model, corrosion is considered as the oxidation of the Pb in the positive electrode grid to PbO_2 and PbO, which leads to a significantly lower conductivity, resulting in resistive losses and a lower density of the oxidized lead, which develops mechanical stress in the positive grid [2]. Thus, corrosion leads to a loss of capacity not only through an increase in internal resistance but also through the loss of active material. During this corrosion, a layer called the "corrosion layer" is formed with a low conductivity, whose resistance adds to the resistance of the battery [1]. The thickness of the corrosion layer is determined by the corrosion voltage Ucorr.

Calculation of the corrosion voltage

The calculation of the corrosion voltage takes into account the voltage of the positive electrode because corrosion mainly affects the positive electrode [1].

During charging, I > 0 we have

$$U_{corr}(t) = U_{corr,0} - \frac{10}{13} g.DOD(t) + 0,5\rho_C \frac{I(t)}{C_N} + 0,5\rho_C M_C \frac{I(t)}{C_N} \frac{SOC(t)}{C_c - SOC(t)} \tag{5}$$

During the discharge, I < 0 on a:

$$U_{corr}(t) = U_{corr,0} - \frac{10}{13} g.DOD(t) + 0,5\rho_d \frac{I(t)}{C_N} + 0,5\rho_d M_d \frac{I(t)}{C_N} \frac{DOD(t)}{C_d - DOD(t)} \tag{6}$$

Calculation of the thickness of the corrosion layer

The principle of calculation of the corrosion layer is based on the work of Lander [2]. A derivation of his graph of corrosion rate versus voltage is used in the model and is illustrated in the following figure:
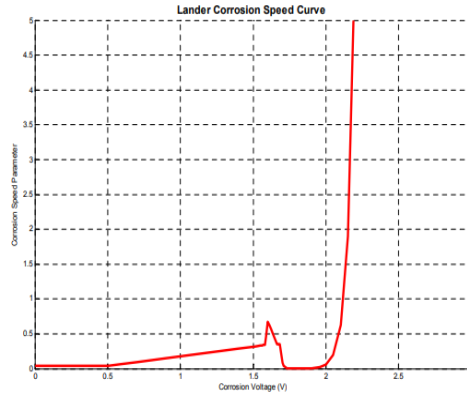
Figure 2: Corrosion rate as a function of corrosion voltage [2]

The corrosion rate accelerates with increasing corrosion stress. According to Lander, the corrosion voltage was the key factor to evaluate the corrosion growth and its speed [2].

For U_{corr} (t) < 1.74 we have

$$\Delta w(t) = K_s . x^{0,6} \tag{7}$$

Where

$$x = \left(\frac{\Delta w(t-\Delta t)}{K_s}\right)^{\frac{1}{0,6}} + \Delta t \tag{8}$$

For U_{corr} (t) ≥ 1.74 we have

$$\Delta w(t) = \Delta w(t - \Delta t) + K_s . \Delta t \tag{9}$$

Δt: Is the duration of a time step and K_s the corrosion rate parameter it is calculated according to the Arrhenius law:

$$K_s(U_{corr}, T) = K(U_{corr}). \exp\left[K_{s,T}.\left(T - T_{corr,0}\right)\right] \tag{10}$$

K(U_{corr}) is a corrosion rate/voltage curve (figure 1.2) based on the work of Lander , $K_{(s,T)}$ is the temperature factor $K_{s,T}$= ln2/15, $T_{corr,0}$ = 298K is the reference temperature.

1.2.1.3. Calculation of the resistance of the corrosion layer and the loss of capacity due to corrosion

The resistance of the corrosion layer and the loss of capacity due to corrosion are all proportional to the ratio of the corrosion layer and the depth of the corrosion layer [1].

- Corrosion layer strength

$$\rho_{corr}(t) = \rho_{corr,lim} . \frac{\Delta w(t)}{\Delta w_{lim}} \tag{11}$$

ρ (corr,lim) is the increase in internal resistance found at the end of the battery's lifetime [1].

$$\rho_{d,fin} = \rho_{d,0} + \rho_{corr,lim} \tag{12}$$

where ρ (d,fin) is calculated from the rearranged Schiffer equation [2] :

$$\rho_{corr,limit} = \left(\frac{C_N}{I(t)}(U - U_0 + g.DOD) - \frac{\rho_d.M_d.DOD}{C_d-DOD}\right) - \rho_{d,0} \tag{13}$$

Capacity due to corrosion

The loss of capacity due to corrosion at a given time is calculated as the initial capacity minus the capacity-reducing effect of corrosion up to that time [2].

$$C_{d,t} = C_{d,0} - C_{corr,t} \tag{14}$$

$$C_{corr}(t) = C_{corr,lim} . \frac{\Delta w(t)}{\Delta w_{lim}} \tag{15}$$

$$C_{corr,lim} = C_{ini} - \left[DOD(t) + \left(\frac{\frac{I(t)}{C_N}.\rho_d.M_d.DOD}{U-U_0+g.DOD(t)+\rho_d.\frac{I(t)}{C_N}}\right)\right] \tag{16}$$

- Calculation of Δw_{lim}

Δw_{lim} is defined as the thickness of the corrosion layer, when the battery reaches its end of life, i.e., at the end of the service life. To calculate Δw_{lim}, the manufacturer's lifetime is multiplied by the corrosion rate parameter ks,limit taken from the k-curve (Ucorr) at voltage Ucorr = Ufloat :

$$\Delta w_{lim} = L. K_{S,lim} \tag{17}$$

With L: the manufacturer's lifetime in years and $K_{S,lim}$ the corrosion rate parameter. Ufloat is the voltage given by the manufacturer in the data sheet.

Degradation model of the active material
Degradation leads to a loss of efficiency of the active material and can also lead to a loss of the active material itself which means a reduction of the battery capacity [2].

Calculation of the cycle number
The nominal cycle number is the number of times the battery has been discharged [2]. Its mathematical expression is as follows [1].

$$Z_N = \int_0^t \frac{|I_{dch}|}{C_N} d\tau \tag{18}$$

With I_{dch} the discharge current.

Capacity loss due to degradation
For the calculation of capacity loss due to degradation, the Ah flow rate is weighted by the impact of state of charge, discharge current and acid stratification. The weighted cycle number is calculated by the following formula [1]:

$$Z_W = \frac{1}{C_N} \int_0^t |I_{dch}(\tau)| . f_{SOC}(\tau) . f_{acide}(\tau) . d\tau \tag{19}$$

$f_{SOC(\tau)}$: is the factor influencing the state of charge which also includes the rate of the current.
$f_{acid(\tau)}$ is the factor of acid stratification.

Impact of the state of charge
The degradation increases with decreasing state of charge. The lower the state of charge, the greater the impact on the lifetime (this is caused by the depth of discharge and the increase in crystal size). The influence of the state of charge is determined by the following formula [1]:

$$f_{SOC}(t) = 1 + (C_{SOC,0} + C_{SOC,min} . (1 - SOC_{min}(t))) . f_I(I, n) . \Delta t_{SOC}(t) \tag{20}$$

$f_{SOC(t)}$ is taken equal to 1 at each full load and increases with time;

$$\Delta t_{SOC}(t) = t - t_0 \tag{21}$$

Where t_0 is the time of the last full charge and SOC_{min} is the lowest state of charge since the last full.
$C_{SOC,0}$ and $C_{SOC,min}$ represents the increase of $f_{SOC(t)}$ at SOC=0.
$f_I(I,n)$, the current factor which describes the influence of the current.
The total factor of the load current is calculated by the formula:

$$f_I(I, n) = f_I(I) . \sqrt[3]{\frac{z(0)}{z(n)}} = f_I(I) . \sqrt[3]{\exp\left(\frac{n(t)}{3,6}\right)} \tag{22}$$

With $f_I(I) = \sqrt{\frac{I_{ref}}{I}}$

The current factor reflects the effect of the lead sulfate crystals. This factor depends mainly on the current at the beginning of the charge. If the battery is initially charged to a SOC strictly between 0.9 and 1 the charge is bad because the number of crystals decreases while their size increases [1].

The number n of bad charges increases each time the SOC reaches a state defined as full charge state generally SOClimit = 0.9 (SOClimit < SOC). Cycles between SOClimit and 1 are not counted as full load so they are considered bad load. When the SOC reaches 1, n is reset to 0 and this load is considered complete. In order to take into account the quality of the charge, we count the number of bad charges with the following assumptions:

- Charging to an SOC of less than 0.9 does not affect the number of crystals and should not be considered a bad charge.
- Dissolving a small number of crystals does not significantly influence the total number of crystals. A significant influence on the number of crystals is only detectable if a significant number of crystals are dissolved [1].

$$n(t + \Delta t) = n(t) + \Delta n = n(t) + \frac{0.0025 - (0.95 - SOC_{max})^2}{0.0025} \tag{23}$$

Impact of acid stratification

The concentration of the electrolyte changes as part of the chemical processes that take place when the battery is charged and discharged [2].

The degree of stratification is given by the formula

$$f_{stra} = \int (f_{plus} - f_{min})dt \tag{24}$$

f_plus and f_min Are the increase and decrease in acid stratification, respectively.

The impact of acid stratification on the degradation of the active ingredient is modeled by the following formula. It is inversely proportional to the current rate [1]:

$$f_{acide} = 1 + f_{stra}\sqrt{\frac{I_{ref}}{|I(t)|}} \tag{25}$$

> The acid stratification increase factor $f_{plus}(t)$

Acid stratification increases during cyclic operation of the battery. The lower the state of charge, the more acid stratification is eliminated and the higher the discharge current. The elimination of acid stratification is assumed to occur due to high gassing. Taking into account all the factors described above, the acid stratification enhancement factor becomes [1]:

$$f_{plus}(t) = C_{plus}.\left(1 - SOC_{min}(t)\right).\exp\left(-3.f_{stra}(t)\right).\frac{|I_{dch}(t)|}{I_{ref}} \tag{26}$$

> The acid stratification decrease factor.

Acid stratification is removed by diffusion and gassing.

> The decrease of acid stratification by gassing

The elimination of acid stratification by gassing begins at voltages above 2.3V/cell and the acid stratification decrease factor increases exponentially [1]. The mixing of the electrolyte is proportional to the amount of gas generated in the battery. Gas generation increases exponentially with voltage and temperature [1].

For a voltage below 2.3V the amount of gas generated in the battery is very small to efficiently mix the electrolyte.

The decrease in acid stratification by gassing is calculated by the following formula [1]:

$$f_{min,gaz} = C_{min}.\sqrt{\frac{100Ah}{C_N}}.\frac{I_{gaz}(t)}{I_{gaz,0}}.\exp\left[C_U.\left(U - U_{ref}\right) + C_T.\left(T - T_{gaz,0}\right)\right] \tag{27}$$

U, the cell voltage

The factor is designed to be equal to C_{min}= 0.1 if U=U_{ref}=2.5V and T=$T_{gas,0}$ for a 100Ah battery. Acid stratification is more difficult to eliminate in large batteries which leads to weighting the gassing with the nominal capacity of the battery.

- Reduction of acid stratification by diffusion

Diffusion is slow, so it is usually only noticeable during long pauses.

It is assumed that the average value of diffusion distance is z/2 and assuming a dependence of temperature on Arrhenius law we have:

$$f_{min,diff} = \frac{2D}{\left(\frac{z}{2}\right)^2}.f_{stra}.2^{\frac{T-20°C}{10}} \tag{28}$$

$$f_{min,diff} = \frac{8D}{z^2}.f_{stra}.2^{\frac{T-20°C}{10}} \tag{29}$$

The acid stratification decrease factor is:

$$f_{min} = f_{min,gaz} + f_{min,diff} \tag{30}$$

The capacity loss due to degradation is calculated by [1]:

$$C_{dég}(t) = C_{dég,lim}.\exp\left[-C_z\left(1 - \frac{Z_w(t)}{1,6.Z_{IEC}}\right)\right] \tag{31}$$

$C_{deg,lim}$, the capacity at the end of life ;

Z_{IEC}, the number of cycles under standard conditions and $C_z = 5$

Temporal evolution of the parameters affected by aging

At the end of each step of the simulation, the new parameters of the battery are calculated.

The increase of the ohmic resistance of the charge and discharge is caused by the resistance of the corrosion layer we have:

$$\rho_c(t) = \rho_c(0) + \rho_{corr}(t) \tag{32}$$
$$\rho_d(t) = \rho_d(0) + \rho_{corr}(t) \tag{33}$$

Calculation of the remaining capacity of the battery

The remaining capacity of the battery is equal to the initial capacity minus the capacity losses due to corrosion and degradation of the active material [1].

$$C_{rest} = C_{ini}(0) - C_{corr}(t) - C_{dég}(t) \tag{34}$$

Improvement of the Schiffer model by imorou and al

- **Determination of the internal operating temperature of the batteries**

Because of the heat transfer phenomena and chemical reactions involved in an electrochemical battery, its internal temperature is quite different from that of the ambient environment [3]. The relation that allows to estimate the operating temperature of the battery is:

$$T = T_a + \Delta T \tag{35}$$

With Ta the ambient temperature and ΔT the temperature variation related to internal heat losses, this variation is determined by the model developed by Copetti and Chenlo [3], given by the relation 36.

$$\Delta T = \frac{c_T}{0.005(C_{10}*1.67)} - \frac{1}{0.005} \tag{36}$$

The maximum capacity CT = 1.7* C10 is estimated. The model of autonomous PV system used in this work is installed in Cotonou, Benin. The system consists of two batteries, a PWM charge controller, an inverter and a PV generator of 3 modules of 200Wp.

Table 1: Data of the installed equipment

Equipements installés	Nombre
Panneau solaire PV VICTRON polycristallin 200Wc/24V	3
Batterie Victron AGM 150Ah/12V	2
Régulateur PWM Shunt de 20A/12- 24 -48V	1
Onduleur AC/DC Pur sinus Victron 800W/24-230V	1

The distribution of expenses is as follows

Table 2 : Profil d'utilisation

Appareil	Nombre	Puissance	Tranche d'heure d'utilisation
Lampes fluorescentes1	10	11W	00h à 7h et 19h à 24h
Lampe fluorescente2	5	11W	05h à 7h et 19h à 24h
Télévision	1	110W	20h à 24h
Prise pour charge portable	1	12W	10h à 14h
Radio cassette	1	16W	12h à 15h et 20h à 24h

This load distribution allows us to have an hourly distribution profile of the power and current consumed.

Results and Analysis

The modeling is done in the Matlab environment, according to the models described previously. The aim is to estimate the end of life of the battery and to study the influence of the temperature on its performance.

Voltage and state of charge of the battery

The current profile of the load supplied by the system under study is represented by the figure 3, this current profile is obtained by considering the operating ranges defined in the table 2.
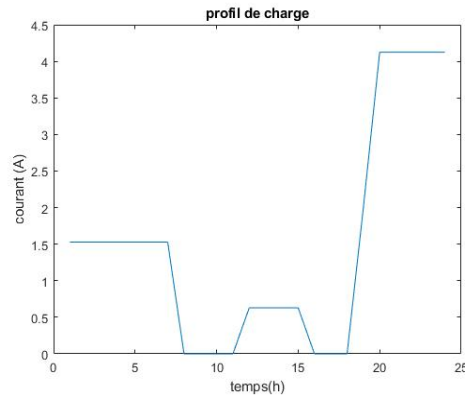

Figure 3: Profile of the battery charge/discharge current over 48 hours

On the curve, the current sometimes takes positive values and sometimes negative values. The negative values of the battery indicate when it is under load (discharging) and the positive values indicate that the battery is charging.

The charge/discharge current profile is used to determine the cell voltage according to Schiffer's equations and the battery's state of charge characterizing the battery's performance. Figure 4 shows the 24-hour battery voltage profile.
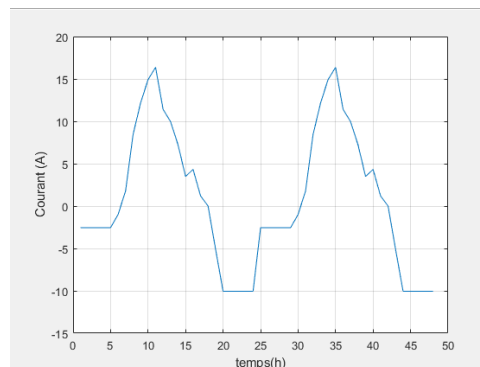

Figure 4: Profile of the battery charge/discharge current over 48 hours

On the curve, the current sometimes takes positive values and sometimes negative values. The negative values of the battery indicate when it is under load (discharging) and the positive values indicate that the battery is charging.

The charge/discharge current profile is used to determine the cell voltage according to Schiffer's equations and the battery's state of charge characterizing the battery's performance. Figure 5 shows the 24-hour battery voltage profile.
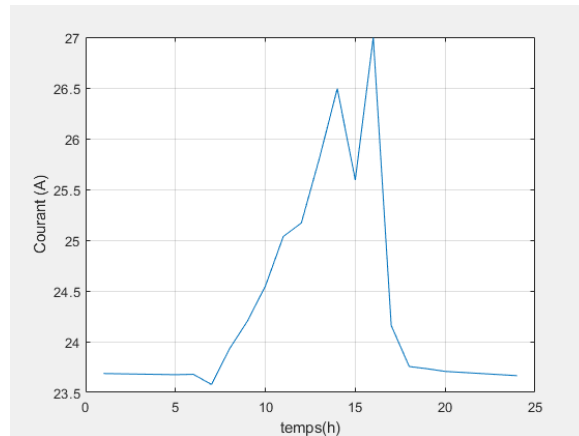
Figure 5: Battery voltage profile over 24 hours

The profile shows that the battery terminal voltage reaches its maximum during the day at 16:00 and does not generally fall below 23.5V, which is well above the critical deep discharge threshold of 21.6V that should not be reached. Figure 6 shows the state of charge of the battery.
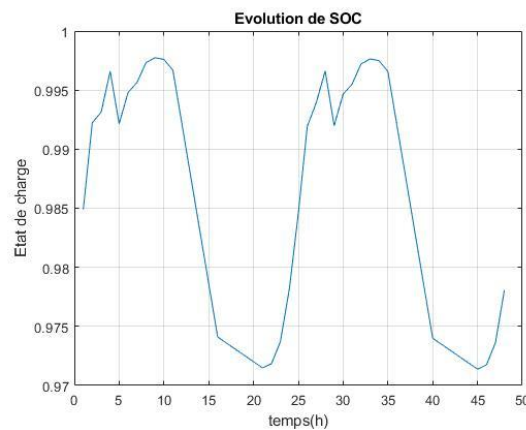

Figure 6: Battery state of charge profile

The battery voltage and state of charge will be used to determine the corrosion and degradation parameters. Figure 7 shows the evolution of the battery capacity during 5 years of operation.
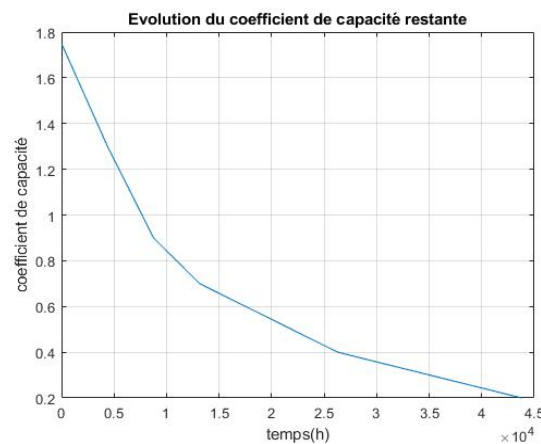

Figure 7: Evolution of the capacity during 43800 hours

After analysis of the curve, we can see that after 3*104 hours or 3 years 153 days of operation, the capacity coefficient of the battery drops from 1.75 to 0.35 or 20% of the initial capacity coefficient. Since the battery reaches its end of life when the remaining capacity coefficient is equal to 20% of the initial capacity coefficient, we conclude that this battery is at the end of its life after 3 years 153 days of operation.

2.2. Influence of temperature on voltage, state of charge and capacity

           ➢   The battery voltage

Figure 8 shows the distribution of the voltage at the terminals of the battery during its operation under three different temperatures, T= 30°C, T=40°C, T= 50°C.
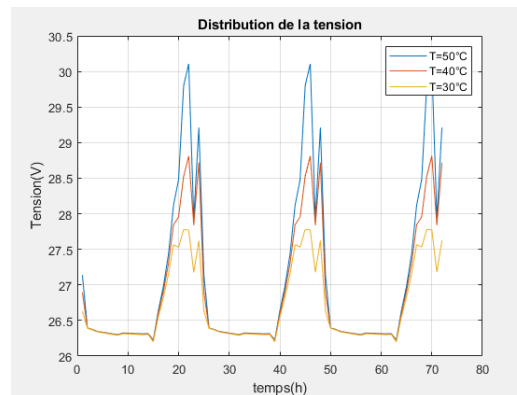

Figure 8: Evolution of the voltage at various temperatures

After analyzing the curve, the voltage at the battery terminals increases when the ambient temperature increases. This increase in voltage will cause excessive outgassing and therefore water loss and corrosion of the positive lead plates.

           ➢   State of charge of the battery

Figure 9 also shows the distribution of the state of charge of the battery during operation at three different temperatures, T= 30°C, T=40°C and T= 50°C
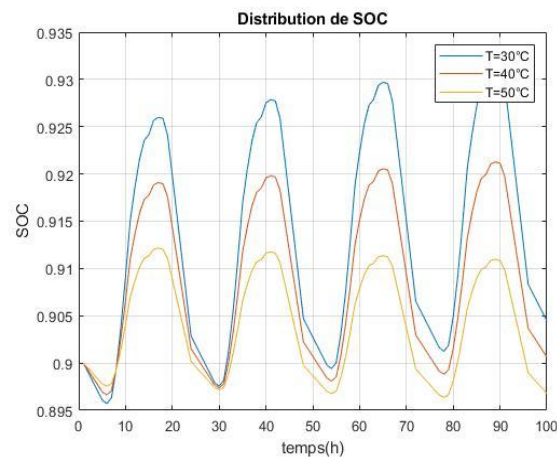

Figure 9: Evolution of SOC at various temperatures

It can be seen that the state of charge of the battery decreases as the temperature increases. At high temperatures the batteries will have difficulty reaching full charge.

Figure 9 shows the evolution of the battery's capacity during its operation at different temperatures.
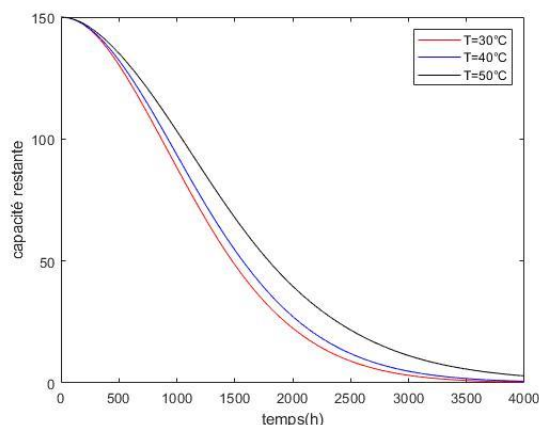
Figure 9: Evolution of capacity at various temperatures

It can be seen that the higher the temperature, the higher the capacity, which means that the battery degrades less quickly at higher temperatures.

Discussion

The battery data sheet shows the rated life of Victron batteries in floating use and as a function of temperature. The life of the AGM battery is 7 to 10 years at a temperature of 20°C. For a temperature of 25°C we obtained a lifetime of 3 years 153 days. The results obtained underestimate the life of the battery, and this is due to the non-respect of the conditions of use of the battery. The results also show that temperature has a negative influence on the performance (voltage and state of charge) of the battery. According to our results, when the temperature increases, the battery has difficulty in reaching maximum loads, the results of YAYA NADJO et al [5] who studied the performance of lead-acid batteries confirm our results. Finally, we found that at high temperatures the capacity of the battery increases and this result is supported by the technical data sheet of the battery. However, under no circumstances should these batteries be placed in a hot location to take advantage of this increase in capacity. The side effects mentioned above are much more harmful.

Conclusion

The main objective of this paper is to develop a simulation tool to predict the lifetime of a battery under real operating conditions. This study based on the capacity weighted aging model allows to study the battery while taking into account the causes of aging in time such as the corrosion of the electrodes and the degradation of the active material. The battery must be integrated in a whole system for its study. The simulation of the models was carried out using a Matlab program. It emerges globally from this study that over 5 years of simulation, the battery studied reaches its end of life at 3 years 153 days of operation and that the temperature is part of the factors that negatively influence the life of the battery including the load and the voltage at its terminals. This study offers many other possible long-term perspectives. It would therefore be interesting to address in future work:

- The implementation of an experimental validation,
- The economic analysis of the battery life on the cost of the whole system.

References

[1]. J. Schiffer, D. U. Sauer, H. Bindner, T. Cronin, P. Lundsager, et R. Kaiser, « Model prediction for ranking lead-acid batteries according to expected lifetime in renewable energy systems and autonomous power-supply systems », *J. Power Sources*, vol. 168, nº 1, p. 66-78, mai 2007, doi: 10.1016/j.jpowsour.2006.11.092.

[2]. H. Bindner, T. Cronin, P. Lundsager, J. F. Manwell, U. Abdulwahid, et I. Baring-Gould, « Lifetime Modelling of Lead Acid Batteries », p. 82.

[3]. A. Thierry, « Conception d'un outil de dimensionnement optimal et de simulation en milieu réel de systèmes solaires autonomes basés sur la méthode KEG », Mémoire de Master de Recherche en Energies Renouvelables et Habitat, Faculté des Sciences et Techniques, Université de Kara, 2019, p. 97.

[4]. R. Dufo-López, T. Cortés-Arcos, J. S. Artal-Sevil, et J. L. Bernal-Agustín, « Comparison of Lead-Acid and Li-Ion Batteries Lifetime Prediction Models in Stand-Alone Photovoltaic Systems », *Appl. Sci.*, vol. 11, nᵒ 3, p. 1099, janv. 2021, doi: 10.3390/app11031099.

[5]. I. YAYA NADJO, « Etude des performances des batteries plomb-acide dans une installation photovoltaïque », Mémoire de Master de Recherche en Efficacité Energétique et Energies Renouvelable, Ecole Doctorale Science de l'Ingénieur, Université d'Abomey-Calavi.